



Augmenting the therapeutic efficacy of adenosine against pancreatic cancer by switching the Akt/p21-dependent senescence to apoptosis

Dongqin Yang^{a,*}, Qi Zhang^{a,1}, Yunfang Ma^a, Zhihui Che^a, Wenli Zhang^a, Mengmeng Wu^a, Lijun Wu^b, Fuchen Liu^c, Yiwei Chu^d, Wei Xu^d, Mary McGrath^e, Chunhua Song^e, Jie Liu^{a,*}

^a Department of Digestive Diseases of Huashan Hospital, Fudan University, Shanghai, China

^b Department of Library, Fudan University, Shanghai, China

^c The Third Department of Hepatic Surgery, Eastern Hepatobiliary Surgery Hospital, Second Military Medical University, Shanghai, China

^d Department of Immunology of School of Basic Medical Sciences, Fudan University, Shanghai, China

^e Department of Pediatrics, Pennsylvania State University College of Medicine, Hershey, PA 17033, USA

ARTICLE INFO

Article history:

Received 20 May 2019

Received in revised form 20 August 2019

Accepted 28 August 2019

Available online 5 September 2019

Keywords:

Adenosine

Akt-p21 axis

Pancreatic cancer

GSK690693

ABSTRACT

Background: There are many reports of the anti-tumour effects of exogenous adenosine in gastrointestinal tumours. Gemcitabine, a first line agent for patients with poor performance status, and adenosine have structural similarities. For these reasons, it is worth exploring the therapeutic efficacy of adenosine and its underlying mechanism in pancreatic cancer.

Methods: Tumour volumes and survival periods were measured in a patient-derived xenograft (PDX) model of pancreatic cancer. The Akt-p21 signalling axis was blocked by p21 silencing or by the Akt inhibitor GSK690693. The combined effect of GSK690693 and adenosine was calculated by the Chou-Talalay equation and verified by measuring fluorescent areas in orthotopic models.

Findings: Among the PDX mice, the tumour volume in the adenosine treatment group was only 61% of that in the saline treatment group. Adenosine treatment in combination with the Akt inhibitor, GSK690693, or the silencing of p21 to interfere with the Akt-p21 axis can switch the senescence-to-apoptosis signal and alleviate drug resistance. A GSK690693-adenosine combination caused 37.4% further reduction of tumour fluorescent areas in orthotopic models compared with that observed in adenosine monotherapy.

Interpretation: Our data confirmed the therapeutic effect of adenosine on pancreatic cancer, and revealed the potential of Akt inhibitors as sensitization agents in this treatment.

Fund: The work is supported by grants from the National Natural Science Foundation of China to Dongqin Yang (81572336, 81770579) and Jie Liu (81630016, 81830080), and jointly by the Development Fund for Shanghai Talents (201660).

© 2019 The Authors. Published by Elsevier B.V. This is an open access article under the CC BY-NC-ND license (<http://creativecommons.org/licenses/by-nc-nd/4.0/>).

1. Introduction

Pancreatic cancer, with its higher mortality-to-prevalence rate than other tumours, was estimated to be responsible for approximately 330,400 new deaths worldwide in 2016, posing a non-negligible threat to public health [1–3]. Numerous drugs have been developed to treat pancreatic cancer, among which gemcitabine has been reported to provide considerable clinical benefit compared to all of the known anti-tumour drugs [4,5]. According to an early trial, 23.8% of pancreatic cancer patients had a clinical benefit with gemcitabine treatment, while it was only 4.8% among patients treated with 5-FU [6].

However, the tumour response rate to gemcitabine is still only 5.4%, far from satisfactory. Severe adverse effects, including bone marrow suppression and fatigue, were also observed in gemcitabine-treated patients in clinical practice, especially in those with cachexia caused by advanced disease progression [7,8]. Moreover, pancreatic cancer has been reported to be capable of limiting its drug absorption by activating metabolic enzymes to break down the drugs, blocking their membrane transporters, and constructing a special tumour micro-environment with a dense stroma and hypoperfusion that impairs drug uptake [9–11]. Therefore, it is necessary to develop novel drugs for treatment of pancreatic cancer with better therapeutic potential and milder adverse effects.

Adenosine is a connatural nucleoside ubiquitously present in most living creatures and is composed of β-N9-glycoside-linked adenine and ribose. Adenosine can be generated from the dephosphorylation of

* Corresponding authors.

E-mail addresses: kobesakura@fudan.edu.cn (D. Yang), jieliu@fudan.edu.cn (J. Liu).

¹ These authors contributed equally to this work.

Research in context

Evidence before this study

Pancreatic cancer is known for its rapid progression and poor prognosis. The connatural nucleoside adenosine regulates metabolism homeostasis as well as various signalling pathways in cancer cells, and shares a similar structure and the same ENT/CNT transporter system with gemcitabine, which is widely used as a chemotherapeutic drug for pancreatic cancer patients with poor performance status. However, the function of adenosine in pancreatic cancer is still unknown.

Added value of this study

We suggest that exogenous adenosine has a potential therapeutic efficacy against pancreatic cancer, and we provide new mechanistic insights into the contradictory role of Akt/p21-axis-mediated senescence in adenosine treatment, which may contribute to the drug resistance of pancreatic cancer.

Implications of all of the available evidence

Our findings confirm the therapeutic effect of adenosine against pancreatic cancer and reveal the potential of Akt inhibitors as sensitization agents for this treatment.

extracellular ATP by CD39 and CD73, by intracellular s-adenosyl-homocysteine hydrolysis, and through *de novo* purine biosynthesis [12]. Since adenosine is a hydrophilic polar molecule that is incapable of penetrating the cell membrane *via* passive distribution, the equilibrative nucleoside transporters (ENT) and concentrative nucleoside transporters (CNT) maintain a dynamic exchange between the extracellular and intracellular sources of adenosine [13,14]. As a vital component of purinergic signalling, adenosine along with its metabolites, inosine and cAMP, can participate directly in the regulation of metabolism homeostasis and DNA replication. They can also affect diverse protein signalling pathways through the G-protein-coupled-cell-surface adenosine receptor family (A1, A2a, A2b, and A3) as an extracellular ligand [15–18].

Previous studies have found exogenous adenosine and its analogues significantly suppress the growth of tumours in the liver, colon, stomach and haematological system [19–22]. *Via* the A3 receptor, exogenous adenosine is able to trigger the caspase-8-mediated extrinsic apoptotic pathway by inducing TNFR1/TRAIL2/FADD upregulation in the liver and in thyroid cancer cells [23]. The activation of A2a, A2b, and A3 receptors can also modulate the profile of Bcl-2 family members for the synergic activation of the caspase-9-mediated intrinsic apoptotic pathway [23,24]. In liver cancer cells, extracellular adenosine can induce AMID-related apoptosis in a caspase and receptor-independent manner [25].

Given the above evidence, we sought to examine the potential therapeutic efficiency of adenosine against pancreatic cancer *in vitro* and *in vivo* to determine the underlying mechanism by which adenosine functions in pancreatic tumours, and to explore the possible mechanism of adenosine-resistance in pancreatic cancer cells.

2. Materials and methods

2.1. Cell culture and reagents

The human pancreatic cancer cell lines SW1990 and BxPC-3 were obtained from the Type Culture Collection of the Chinese Academy of

Sciences (Shanghai, China). The cells were cultured in Dulbecco's modified Eagle's medium containing 10% foetal bovine serum (Thermo Fisher Scientific) and 1% penicillin-streptomycin at 37 °C with 5% CO₂. Adenosine (018–10,492) was purchased from Wako (Osaka, Japan) and 8-CPT (#C0735), DMPX (#D134), alloxan (#A7413), MRS1523 (#M1809), EHNA (#E114), forskolin (#F6886), SQ22536 (#S153), H89 (#B1427), and dipyridamole (#D9766) were purchased from Sigma (Shanghai, China); HPBCD (#A600388) was from Sangon Biotech (Shanghai, China); and GSK690693 (#HY-10249) was from MCE (New Jersey, USA). For *in vivo* studies, adenosine and GSK690693 were dissolved in 10% 2-hydroxypropyl-β-cyclodextrin (Sangon Biotech, Shanghai, China).

2.2. Immunoblotting

The cell lysates were extracted with cell lysis buffer (Beyotime, China); a total amount of 20–50 μg of each sample was submitted to immunoblotting and detected by antibodies that recognize c-caspase 3 (#9661, RRID: AB_2341188), c-caspase 8 (#9496, RRID: AB_561381), c-caspase 9 (#9509, RRID: AB_2073476), PARP (#5625, RRID: AB_10699459), p21 (#2947, RRID: AB_823586), pAkt (#5625, RRID: AB_2315049), pRb (#9313, RRID: AB_1904119); p16 (#92803, RRID: AB_2750891) (Cell Signalling Inc., Danvers, MA, USA); and actin (#CW0096, CWBIO, China).

2.3. RNA interference

The pancreatic cancer cells were distributed in the 60-mm plate with a concentration of $0.5 \times 10^6/5$ ml and 18–24 h later they were transfected with Lipofectamine RNAiMax (#13778500, Invitrogen, Carlsbad, CA, USA), siRNA oligonucleosides were synthesized by RIBOBIO (Guangzhou, China) as we previously reported [26]. Separately, siRNA and Lipofectamine RNAiMax were incubated with Opti-MEM (#31985088, Invitrogen, Carlsbad, CA, USA) for 5 min and then mixed together for 20 min at room temperature. The mixture was applied to the cells. The final concentration of siRNA reached 50 nM. The siRNA for p21 was obtained from CST (#6456, Danvers, MA, USA).

2.4. SA-β-Galactosidase staining

The cells were distributed in the 6-well plate with a concentration of $1 \times 10^5/ml \times 2$ ml and treated with adenosine or transfected with sip21 (final concentration of siRNA is 50 nM) for 72 h. The expression of senescence-associated β-Galactosidase was determined with the SA-β-Galactosidase (SA-β-Gal) staining kit (#94433, Sigma, St. Louis, MO, USA) according to the manufacturer's specifications as we previously reported [26].

2.5. FACS analysis

The cells were distributed in the 6-well plate with a concentration of $2 \times 10^5/ml \times 2$ ml and treated with the indicated concentration of adenosine for 72 h. According to the manufacturer's instructions, apoptosis was detected with the Annexin V-FITC/PI Apoptosis Kit (#K101, BioVision, Inc. Milpitas, California), and the activity of caspase-3 was measured using a CaspGLOW assay kit (#K183, BioVision, Inc., Milpitas, California, USA).

2.6. Combination index analysis

For the combination index (CI) analysis, the 3×10^3 cells/1 ml in 96-well plate were treated with a concentration gradient of adenosine, GSK690693 or their constant ratio combination for 48 h. The CI value of the combination of adenosine and GSK690693 was calculated according to the Chou-Talalay method by CompuSyn software, with CI >1,

CI = 1, and CI <1 indicating antagonism, an additive effect, and synergism, respectively.

2.7. PDX cohort expansion

Pancreatic ductal adenocarcinoma tissues were derived from the patients (Patient 003, 018, 026 and 031) with localized pancreatic cancer, who had undergone curative surgical resection at Huashan Hospital, Shanghai, China. Written informed consent from all four patients in accordance with the Declaration of Helsinki was obtained, and this study was approved by the Human Ethics Committee of Huashan Hospital.

The patients' tumour tissues were subcutaneously engrafted into the flanks of NSG/NOD mice to be expanded over time. When tumour mass reached 1 cm in diameter, they were isolated and cut into small pieces (1mm³). The small tumour masses were subcutaneously inoculated into the flanks of the 6 to 8-week-old male Nu/nu mice with an average weight of 18–20 g [27,28]. When the engrafted tumours had grown to a median size of 100 mm³ in 7–10 days after inoculation, the mice were randomly divided into the adenosine treatment group or the control group.

For each PDX tumour line, each treatment group was composed of at least three mice, which were to be treated with adenosine by intraperitoneal injection at 50 mg/kg, or with normal saline every 2 days for 6 weeks. The tumour volumes and animal body weights were measured twice per week using callipers or scales. The numbers of dead mice were counted in the adenosine and the control group for calculation of the survival rate of the mouse model. The differences in tumour volume, body weights and survival rates between the treatment groups were statistically significant.

2.8. Orthotopic transplantation tumour model of human pancreatic cancer and immunohistochemical staining

The stable BxPC-3-GFP cells were generated as described [29]. An orthotopic implantation tumour model of pancreatic cancer was established using the BxPC-3-GFP cells as previously reported [29]. Briefly, 10⁷ cells were subcutaneously inoculated into the flanks of BALB/c Nude mice. The tumours, when they reached 1 cm in diameter, were isolated and cut into small pieces (1mm³). Then, the small tumour masses were surgically inoculated on the pancreas tail of the mice (total 40 mice) [30]. The fluorescence in the live animals were detected 7 days after transplantation using an Olympus OV100 imaging system (Corel, Ottawa, ON, Canada). The mice without fluorescent signals detected were removed.

The tumour-bearing mice were randomized into 4 groups: the first group to be treated with 10% 2-hydroxypropyl-β-cyclodextrin (HPBCD), the second group to be treated with adenosine by intraperitoneal administration (i.p.) (50 mg/kg), the third group to be treated with GSK690693 by i.p. (20 mg/kg), and the fourth group to be treated with adenosine (50 mg/kg) and GSK690693 (20 mg/kg). All four groups were treated every other day for 6 weeks. Whole-body images were acquired using an Olympus OV100 imaging system every three days, and the fluorescent intensity of the tumours were quantified. Tumour size was determined by the volume of the fluorescent areas. At the end of the experiment, the tumour tissues were harvested, photographed and weighed. The difference of the tumour size and tumour weight in the four groups were compared and statistically analysed.

Protein expression changes were evaluated through IB analysis using specific antibodies as indicated. Animal experiments were performed in accordance with the animal protocols approved by the Institutional Animal Care and Use Committee of Anti-Cancer Biotech (Beijing, China). The pancreatic cancer tissues were stained with antibodies against Ki-67 (#ab16667, RRID: AB_2315049, Abcam Trading Company Ltd., Shanghai, China) and c-caspase 3 (#9661, RRID: AB_2341188, Cell Signalling, Boston, MA).

2.9. Reverse transcription-polymerase chain reaction analysis

The 30–50 mg tumour tissues that had received a certain treatment were lysed by TRizol (#15596018, Life Technologies, Carlsbad, CA, USA). The RNAs were reversed using PrimeScript RT master mix (#RR036A, Takara) and qPCR was performed by SYBR Premix Ex Tag II (#RR820A, Takara, Dalian, China). The level of the target gene's mRNA was normalized to that of the reference gene, actin. A list was made of the primers as follows:

ENT1: F-CAGCCTGTGCAGTTGTCATT, R- CCGTGAA GATGAAGCAGA CA,

ENT2: F-TTGCCCGTTACT ACCTGACC, R- CGACAGGGTGACTGTG AAGA,

ENT3: F-TAGCAGCTCCTCCACCATCT, R- GGC AACTGGCCTCATGTAGT,

ENT4: F-ACCGCTA CCATGCCATCTAC, R- CCTGGTCGTGAGAGAAG AGC,

CNT1: F-TGGTCTACCCAGAGGTGGAG, R- GGACGTAGGAGCAGAT GAGC,

CNT2: F-ATGCTTGAAGCCTCTGGAAA, R- ATCTGATCTCC CAGCCATTG,

CNT3: F-CAAACCTGGGCCAACAA AACT, R- GGGCAGGATCTTAAAT GCAA,

Actin: F-CCACACCTTCTACAATGAGC, R- GGTCTCAAACATGATCTGGG.

2.10. Cell cycle analysis

Cells were distributed in the 6-well plate with a concentration of 2 × 10⁵/ml × 2 ml and treated with the indicated drugs for 72 h. After harvest, the cells were fixed with 70% ethanol overnight and washed with PBS before incubation with RNase A (#R6513, Sigma, 1.5 µg/ml) for 1 h at 37 °C, followed by staining with 5 µl PI (#P4170, sigma) for 20 min on ice. After that, their DNA content was detected by flow cytometry (Beckman, USA) and analysed using ModFit LT software (Verity Software House Inc., Topshan, USA).

2.11. Statistical analysis

Statistical analysis was performed using GraphPad Prism 6 software (La Jolla, CA, USA). The unpaired two-tail student *t*-test was applied to evaluate the difference between the treatment and non-treatment control group in cell-based assays and the mouse models. The two-way ANOVA with Bonferroni post-test was applied when analyzing the data of multiple groups in the drug combination assays with the mouse model. The continuous dependent variables of each experiment were presented as mean ± SEM unless otherwise specified. The follow-up for the Kaplan–Meier survival curves was started when the engrafted tumours in the PDX mice (*n* = 11) had grown to be the median size of 100 mm³. During the follow-up, the survival statuses of the PDX mice were checked everyday. Then at Day 42 when one of the PDX mice had a tumour volume ≥ 2000 mm³ follow up was ended in order to follow the ethical requirements. The open circles in the curves represent censoring because one mouse in each group was excluded from checking engraftment. A log-rank test was used to analyze the Kaplan–Meier survival curves. The data are expressed as means ± SEM. For all of the tests, four levels of significance were determined: **P* < .05, ***P* < .01, ****P* < .001 and *****P* < .0001.

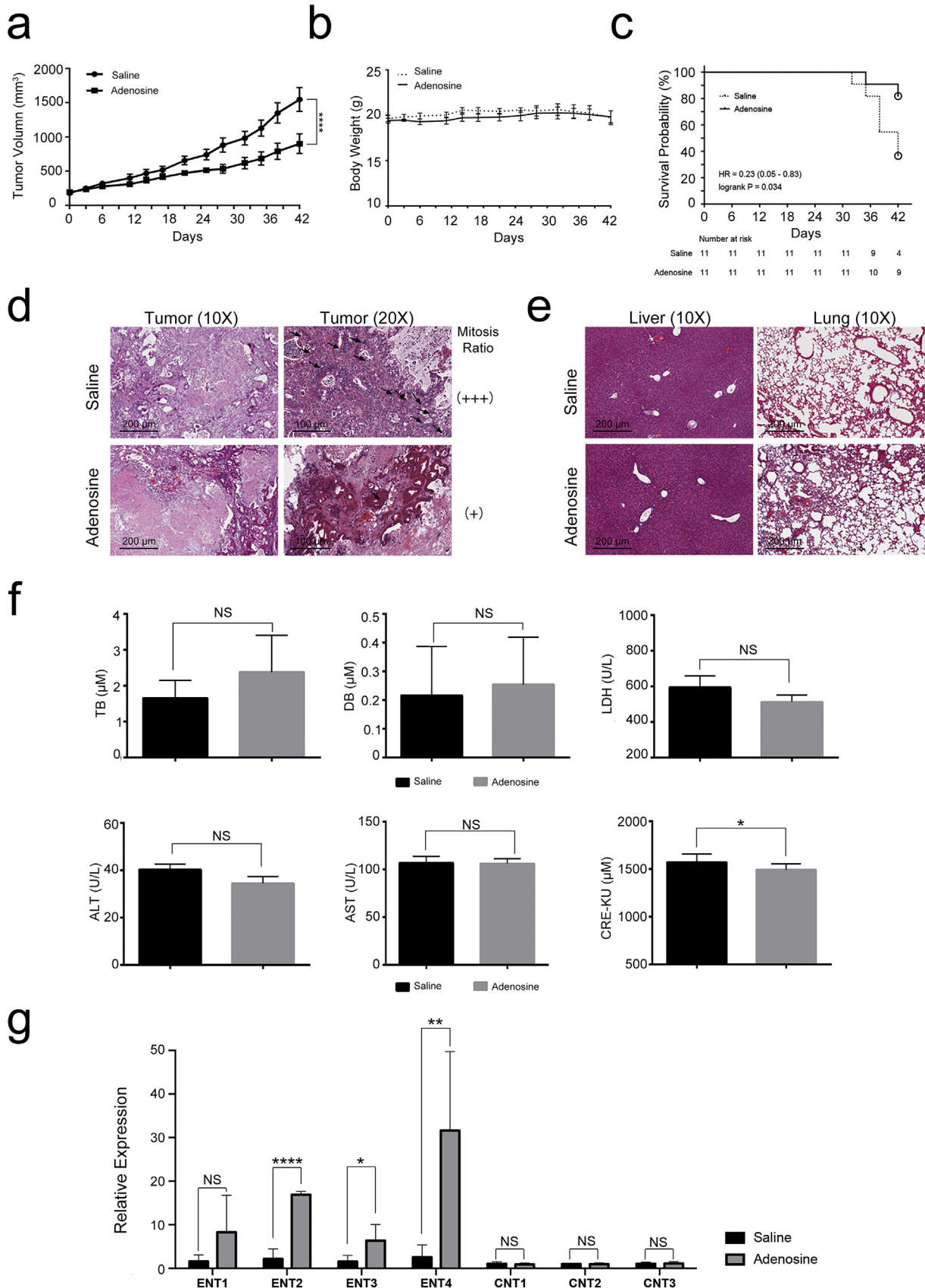
3. Results

3.1. Adenosine exhibits anti-tumour effects on pancreatic cancer in PDX models

The anti-tumour effect of adenosine on multiple cancer cell lines has been documented in previous studies [19–25]. However, whether adenosine shows similar therapeutic efficacy against primary cancer *in vivo* is still unclear. To address this question we generated patient-derived xenograft (PDX) mouse models that bear tumour tissues from 4

different pancreatic cancer patients (Patients 003, 018, 026 and 031). These PDX mice were then treated with adenosine or saline, and the tumour volumes were measured at various time points during the treatment. We found that the tumour growth rate was slowed after the

second treatment with adenosine, and the final average tumour volume was approximately 40% smaller than the saline-treated group (adenosine: $901.1 \pm 381.7 \text{ mm}^3$, saline: $1547.1 \pm 462.8 \text{ mm}^3$, Fig. 1a). There was a significant difference between the two groups ($p < .0001$, two-



AVOVA). A significantly better survival rate was seen in the adenosine-treated group after 42 days of administration ($P < .05$, student *t*-test) (Fig. 1c). The relative decrease in tumour volume might be correlated with a reduced mitotic rate of tumour cells in response to adenosine treatment as shown previously (Fig. 1d).

In spite of a steady decrease in the tumour volumes, the average body weights of the adenosine-treated mice remained stable and were comparable to that in the saline-treated group at all time points tested (Fig. 1b), suggesting the overall toxicity of adenosine is low. This is further supported by the pathological examination and biochemical blood tests of the animals at the end of the treatment. No significant differences in the liver and lung HE-stained sections were observed between the two groups (Fig. 1e). Most of the indicators in the blood biochemistry tests were found to be similar between the two treatments as well, except for LDH. A significant lower LDH ($P < .05$) upon adenosine treatment is consistent with the smaller tumour volume in the adenosine-treated group (Fig. 1f). These results suggest adenosine treatment did not cause major abnormal physiological changes in the PDX models, providing preliminary proof for the clinical safety of adenosine treatment.

One of the major strategies used by pancreatic cancer cells to enhance their tolerance of chemotherapeutic agents is downregulation of the concentrative and equilibrative nucleoside transporters (CNTs and ENTs), which are responsible for the intracellular delivery of nucleosides. We, therefore, tested whether the expression of CNTs and ENTs decreased after adenosine treatment. As shown in Fig. 1g, adenosine significantly increased the expression of ENT2 ($P < .0001$), ENT3 ($P < .05$), and ENT4 ($P < .01$), increasing the effective delivery of adenosine into pancreatic cancer cells. These data together indicate that adenosine can effectively suppress pancreatic cancer cell growth safely, and the ENT family may be involved in adenosine's effect on effectively suppression of pancreatic cancer growth.

3.2. Adenosine exerts anti-tumour effects on pancreatic cancer cells via its transporters

To explore the underlying mechanism by which adenosine suppresses tumour growth, we first examined whether the anti-tumour effect of adenosine is dependent. We chose two canonical pancreatic cancer cell lines, SW1990 and BxPC3, and treated cells with adenosine at different concentrations from 0.01 mM to 10 mM. We observed that at a low concentration from 0.01 mM to 0.1 mM, exogenous adenosine promoted the growth of pancreatic cancer cells slightly. However, as its concentration increased, adenosine strongly inhibited the growth of both the BxPC3 and SW1990 cell lines by 40% and 80%, respectively, after 72 h of treatment. These observations suggest that only at high concentrations does exogenous adenosine exert a tumour-suppressing effect on pancreatic cancer cells (Fig. 2a).

Adenosine can either bind to its receptors on the cell surface, thus triggering downstream signalling pathways, or be absorbed from the extracellular environment and be metabolized into inosine or cAMP, the latter of which is one of the critical second messengers for PKA activation. To determine by which mode adenosine exerts its tumour suppressing effect, we tested whether blocking adenosine receptors could interfere with adenosine function. Addition of a combination of inhibitors for specific adenosine receptors (8-CPT for A1a, DMPX for A2a, alloxan for A2b and MRS1523 for A3) [21,31] did not attenuate the growth inhibition effect of adenosine (Fig. 2b), suggesting adenosine receptors are dispensable for the tumour suppressing effect.

We then determined whether intracellular levels of adenosine are necessary for its function. We disrupted the absorption of adenosine and decreased its intracellular concentration by using dipyrindamole, a pan-inhibitor for all of these transporters [32]. We observed that the viability of both cell lines was remarkably recovered by dipyrindamole in a dose-dependent manner (Fig. 2d), indicating high levels of intracellular adenosine are critical for its anti-tumour effect. In order to confirm the cytotoxicity is mediated by adenosine itself, but not its metabolites, we next incubated the adenosine-treated cells with the adenosine deaminase inhibitor EHNA, the adenylate cyclase agonist forskolin, the adenylate cyclase antagonist SQ22536, or the PKA inhibitor H89 [31,33], and measured the cell viability 72 h post-treatment (Fig. 2c). We found that EHNA significantly increased the cytotoxic effects of adenosine by preventing its metabolism in pancreatic cancer cells. These results implied that the tumour suppressing effect was mediated by the elevated levels of intracellular adenosine.

3.3. Adenosine induced apoptosis in pancreatic cancer cells

Adenosine has been shown to induce apoptosis in several types of cancer cells. To determine whether adenosine suppresses pancreatic cancer cell growth *via* the same mechanism, we examined the rate of apoptosis in SW1990 and BxPC3 cells upon adenosine treatment using Annexin V/PI staining. As shown in Fig. 3a, when the adenosine concentration reached 1 mM, the apoptosis rate increased drastically in the treated cells. We also measured caspase-3 activation using FITC-ZAD-FMK and immunoblotting, and found the level of cleaved caspase-3 correlated with the apoptosis rate as shown in Fig. 3b and Fig. 3c. Similar patterns were also observed for the cleavage of PARP and caspase-9, two additional proteins important in apoptosis. This dosage-dependent pattern of the apoptosis rate was also inversely correlated with the cell growth curves (Fig. 2a), indicating the importance of apoptosis in adenosine treatment.

Moreover, the kinetics of the cleavage of these three proteins revealed that 24-h treatment with adenosine at 1 mM was sufficient to initiate the apoptotic signals. Interestingly, 5 μ M of dipyrindamole was able to retain the cleavage of the three proteins to the same levels as that in the control group and additionally prevented the adenosine-induced growth inhibition (Fig. 3d and 2d). This suggests extracellular adenosine induces cell death, predominantly by apoptosis, *via* an intrinsic pathway relevant to adenosine uptake into pancreatic cancer cells.

3.4. Adenosine treatment induced p21-dependent senescence of pancreatic cancer cells

Treatment with adenosine at 1 mM induced apoptosis in both pancreatic cancer lines; however, a portion of the cells became flattened and attached to the bottom of the petri dish, resembling cellular senescence. Senescence is known as an irreversible status of cell cycle arrest and is characterized by the over-expression of a specific β -galactosidase. We speculated that this senescence-like phenomenon might be another reason to account for the significant decrease of mitotic cells in the tumour biopsies from the adenosine-treated PDX mice. To test whether the cells underwent senescence, we stained SW1990 and BxPC3 cells with SA- β -gal 72 h post adenosine treatment and quantified the staining positive cells under a non-phase contrast microscope. The number of senescent cells in SW1990 and BxPC3 was six times higher than that of untreated cells (Fig. 4a). We also observed an increased percentage of cells in the G2/M phase of the cell cycle,

Fig. 1. Adenosine suppresses tumour proliferation in PDX models. PDX mice derived from 4 unrelated pancreatic cancer patients and treated with adenosine and HPBCD by intraperitoneal administration at 50 mg/kg every 2 days for 6 weeks. **a:** Tumour volume. Error bars indicate SEM; **** $P < .0001$; two-way ANOVA, $n = 11$. **b:** Body weight. $n = 11$. **c:** The comprehensive effect of each treatment on all of the subjects analysed by Kaplan–Meier survival curves. The open circles in the curves represent censoring. Log-rank test, $n = 11$. **d & e:** Biopsies of the tumours, lungs and livers stained by haematoxylin and eosin; the mitotic cells in the tumour biopsies are labelled with black arrows. **f:** The serum level of biochemical indexes measured in each treatment group. Error bars indicate SEM; * $P < .05$; Student's *t*-test, $n = 6$. NS stands for non-significant. **g:** The expression of ENT and CNT family members in tumours detected by real-time PCR. Error bars indicate SEM; * $P < .05$, ** $P < .01$, **** $P < .0001$; Student's *t*-test, $n = 6$. NS stands for non-significant.

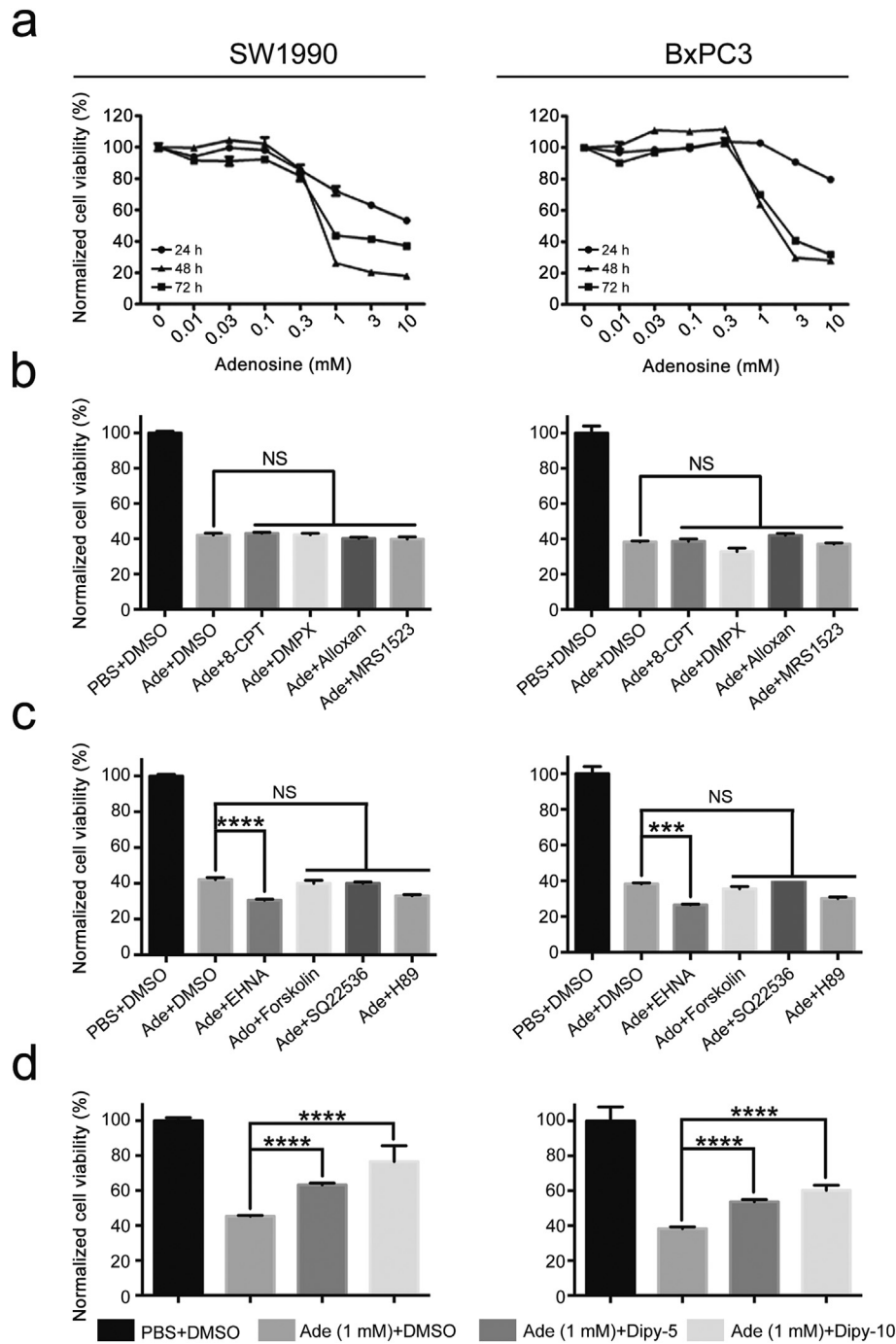
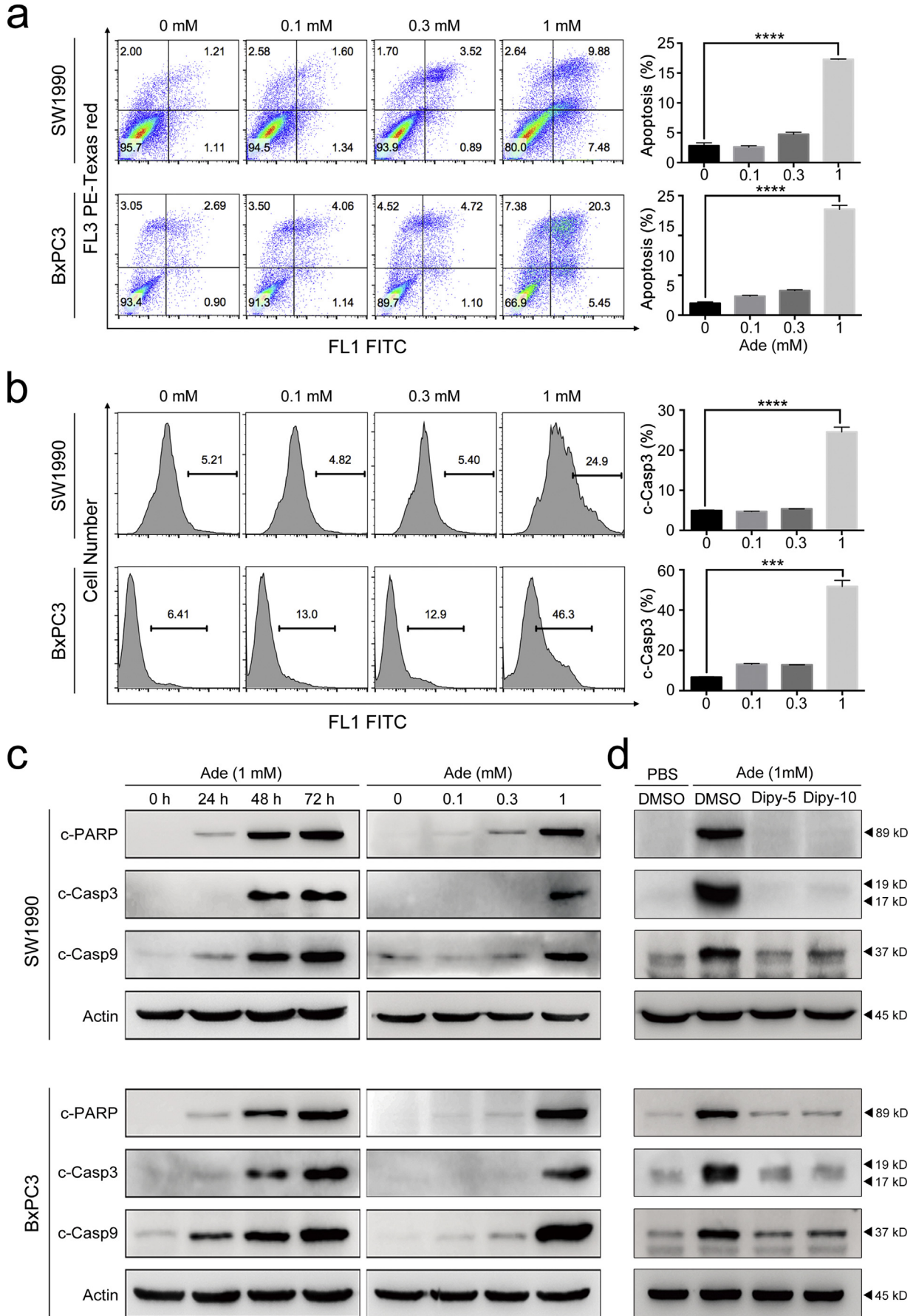


Fig. 2. Adenosine inhibits the growth of SW1990 and BxPC3 cells in a dosage and time-dependent way. **a:** The cell viability measured by MTS assay. **b–d:** The impact of 8-CPT, DMPX, alloxan, MRS1523, EHNA, forskolin, SQ22536, H89 and dipyradomole on the adenosine-treated cells tested by MTS after combined treatments with adenosine. Ade, adenosine; Dipy-5, 5 μ M dipyradomole; Dipy-10, 10 μ M dipyradomole; NS, no significant difference. Error bars indicate SEM; *** P < .001 and **** P < .0001; Student's t -test, n = 3. NS stands for non-significant.

consistent with the senescent-like phenotype observed above (Supplementary Fig. S1). These data indicated that senescence is one of the underlying mechanisms for adenosine-induced inhibition of cell growth in pancreatic cancer.

p21 and p16 are two important members of the Cip/Kip family and INK family and are known to play critical roles in surveying cell cycle progression and interrupting mitosis for error correction during this process. Therefore, we asked whether the expression of these two proteins was affected by adenosine treatment. We determined the levels of these proteins in pancreatic cancer cells treated with adenosine at different concentrations (Fig. 4b). We found that p16 and its downstream target the Rb protein didn't respond to the adenosine treatment

regardless of the treatment duration or drug concentration. In contrast, the p21 protein level increased in the cells treated with adenosine, and it was further upregulated with an increasing amount of adenosine. The adenosine induced expression of p21 was abolished with the addition of dipyradomole (Fig. 4c), indicating that intracellular adenosine is required for the upregulation of p21 in the tumour cells. Given the previous findings that p21 could induce cell cycle arrest at the G2 phase by inhibiting CDK1 phosphorylation, we speculated that p21 mediated adenosine-induced senescence. To test this, we transduced pancreatic cancer cells with siRNA specific for p21 (sip21) or scramble siRNA (siNC) before treating cells with 1 mM adenosine and measuring the cellular senescence at 72 h post-treatment. We found that in both cell



lines, p21 silencing significantly reduced the percentage of the senescent cells after treatment with adenosine (Fig. 4d). Therefore, p21-dependent senescence also contributes to adenosine induced growth inhibition of pancreatic cancer cells.

3.5. Silencing p21 promotes cellular senescence to apoptosis and augments the adenosine sensitivity in pancreatic cancer cells

Adenosine treatment induced both apoptosis and senescence in pancreatic cancer cells, which led us to ask whether there was any interaction between the two cellular processes and how it would affect the response to adenosine treatment. We first measured the cell viability and apoptosis ratio in adenosine-treated pancreatic cancer cells with or without silencing p21. Notably, the viability of cells upon adenosine treatment was further reduced by 10% with p21 silencing, which is consistent with increased activation of caspase-3 in the same cells (Figs. 5a & 5b). Moreover, we also detected increased pro-apoptotic cleavage of PARP by the caspase cascades in the cells with lower p21 expression when treated with adenosine (Fig. 5c).

The above results suggest that downregulation of p21 expression may switch cellular senescence to apoptosis in pancreatic cancer cells, thereby augmenting the cytotoxicity of adenosine in pancreatic cancer cells.

3.6. Sensitization of pancreatic cancer cells to exogenous adenosine by an Akt inhibitor

As a cell cycle regulator, p21 performs various functions that are highly dependent on its subcellular localization. In general, p21 shuttles between the cytoplasm and nucleus, a process that is controlled by the phosphorylation of specific amino acid residues on the p21 protein. Akt is one of the most well studied kinases that can phosphorylate p21. It phosphorylates p21 on Threonine145 or Serine146, which disrupts the p21-PCNA complex and promotes the cytoplasmic localization of p21 [34–36]. It has been previously been reported that the cytosolic p21 can help cells resist apoptosis by binding to pro-apoptotic proteins [37], which is consistent with the current findings. Therefore, we hypothesized that Akt might function upstream of p21 to antagonize adenosine's cytotoxicity in pancreatic cancer cells.

To test this hypothesis, we treated cells with the Akt inhibitor GSK690693 during the adenosine treatment. GSK690693 is an ATP analogue that binds to the catalyzing cleft of Akt, thus blocking its kinase function. When the pancreatic cancer cells were treated with 1 mM adenosine and different amounts of GSK690693, the two cell lines showed different degrees of sensitivity to this inhibitor. Despite this discrepancy, the addition of GSK690693 resulted in a decrease of cell viability by 20% to 30% in both adenosine-treated pancreatic cancer cell lines 96 h post treatment (Fig. 6a and Supplementary Fig. S2).

To determine whether GSK690693 and adenosine treatment have a synergic effect on cells, we designed a series of constant ratio combinations for adenosine and GSK690693, and tested their combined effect using the Fraction Affected–Combination Index plot (Fa-CI plot) according to the Chou–Talalay equation. GSK690693 and adenosine were found to display a synergic effect within certain concentration ranges for either of the medications, although they showed distinct patterns using the Fa-CI plot (Fig. 6b).

Based on these graphs, two appropriate combinations of adenosine and GSK690693 were chosen to treat each cell line for 72 h. GSK690693 significantly alleviated the adenosine-induced p21 upregulation and augmented Akt phosphorylation via a negative feedback loop

as previously reported [38] (Fig. 6c). Moreover, this combination strongly amplified the activation of the apoptotic signals including caspase-3 and PARP in adenosine-treated cells (Fig. 6d). Therefore, the Akt-p21 signalling axis determined the balance between senescence and apoptosis in the adenosine-treated pancreatic cancer cells.

3.7. The potential therapeutic effect of adenosine reinforced by GSK690693 in the murine orthotopic pancreatic cancer model

To further demonstrate the combined effect of adenosine and GSK690693 *in vivo*, we established EGFP-labelled BxPC3 cells and generated a murine orthotopic pancreatic cancer model by transplanting these cells into BALB/c nude mice. These mice were divided into four groups and were treated with one of the following: adenosine (Ado), GSK690693 (GSK), adenosine-GSK690693 mixture (A + G), or vehicles as control (NC).

During the treatment, cancer cell growth as indicated by the fluorescence in the pancreas of each mouse was measured and quantified. The growth of cancer cells in mice treated with adenosine or GSK690693 was significantly suppressed compared with that of the NC group. Additionally, as the treatment was prolonged, the fluorescent area of the A + G group became even smaller than that of the Ado and GSK groups (Figs. 7a–c). The volume of the tumour tissues was measured at the end of the treatment. As shown in Fig. 7b and Fig. 7c, the average tumour volume of mice in the Ado group was significantly reduced to only half of that of the NC group. The average tumour from the A + G treated mice decreased by 32% compared to that of the Ado group, suggesting the improved efficiency of this combined regimen (Figs. 7b & 7d).

To determine whether adenosine suppressed pancreatic cancer growth by inducing apoptosis, we examined caspase-3 cleavage by immunohistochemical staining of the tumour tissue and immunoblotting. While Ki-67 expression, a marker for cell proliferation, was downregulated in samples from all treated groups, the activation of caspase-3 was elevated with the highest level in the A + G group (Fig. 7e). Quantification of protein levels also showed increased expression of caspase-3 and phosphorylated Akt in samples from the A + G group (Fig. 7f). These data demonstrate that the exogenous adenosine could exert a potential therapeutic effect on pancreatic cancer by inducing apoptosis of the cancer cells, and that GSK690693 could further improve the efficacy of adenosine by blocking Akt signalling.

Taking all of the *in vivo* data together, we conclude that exogenous adenosine has potential therapeutic efficacy for pancreatic cancer and that the Akt inhibitor GSK690693 could possibly be used as an applicable sensitizer in the clinical setting.

4. Discussion

In the current study, we demonstrated the anti-tumour effect of exogenous adenosine on pancreatic cancer and validated its potential in clinical application.

Given its wide range of involvement in physiological activities, including heart rhythm adjustment, neural signal transmission, and adipose tissue differentiation, adenosine has long been studied for its impact on tumorigenesis. Previous reports suggested that adenosine from different sources and at different concentrations could carry out distinct functions in cancer cells either through binding to adenosine receptors A2a, A2b, and A3, or through dosage-dependent AMPK activation [39,40]. We observed a similar anti-tumour effect of exogenous adenosine in pancreatic cancer cells. At millimolar concentrations, this

Fig. 3. Adenosine triggers the apoptosis of SW1990 and BxPC3. **a:** The apoptosis induced by adenosine at different concentrations at the time point of 72 h, detected (left panel) and measured (right panel) by PI/Annexin V-FITC staining. **b:** The caspase-3 cleavage triggered by adenosine, detected and measured by FITC-DEVD-FMK staining (left panel); the relative ratios of the cells with the fluorescent intensity, plotted as histograms (right panel). **c:** The levels of caspase-3, caspase-9 and PARP cleavage analysed by immunoblotting. **d:** The levels of caspase-3, caspase-9 and PARP cleavage analysed in SW1990 and BxPC3 cells receiving combined treatment of adenosine and dipyrindamole; Dipy-5, 5 μ M dipyrindamole; Dipy-10, 10 μ M dipyrindamole. Error bars indicate SEM; *** $P < .001$ and **** $P < .0001$; Student's *t*-test, $n = 3$.

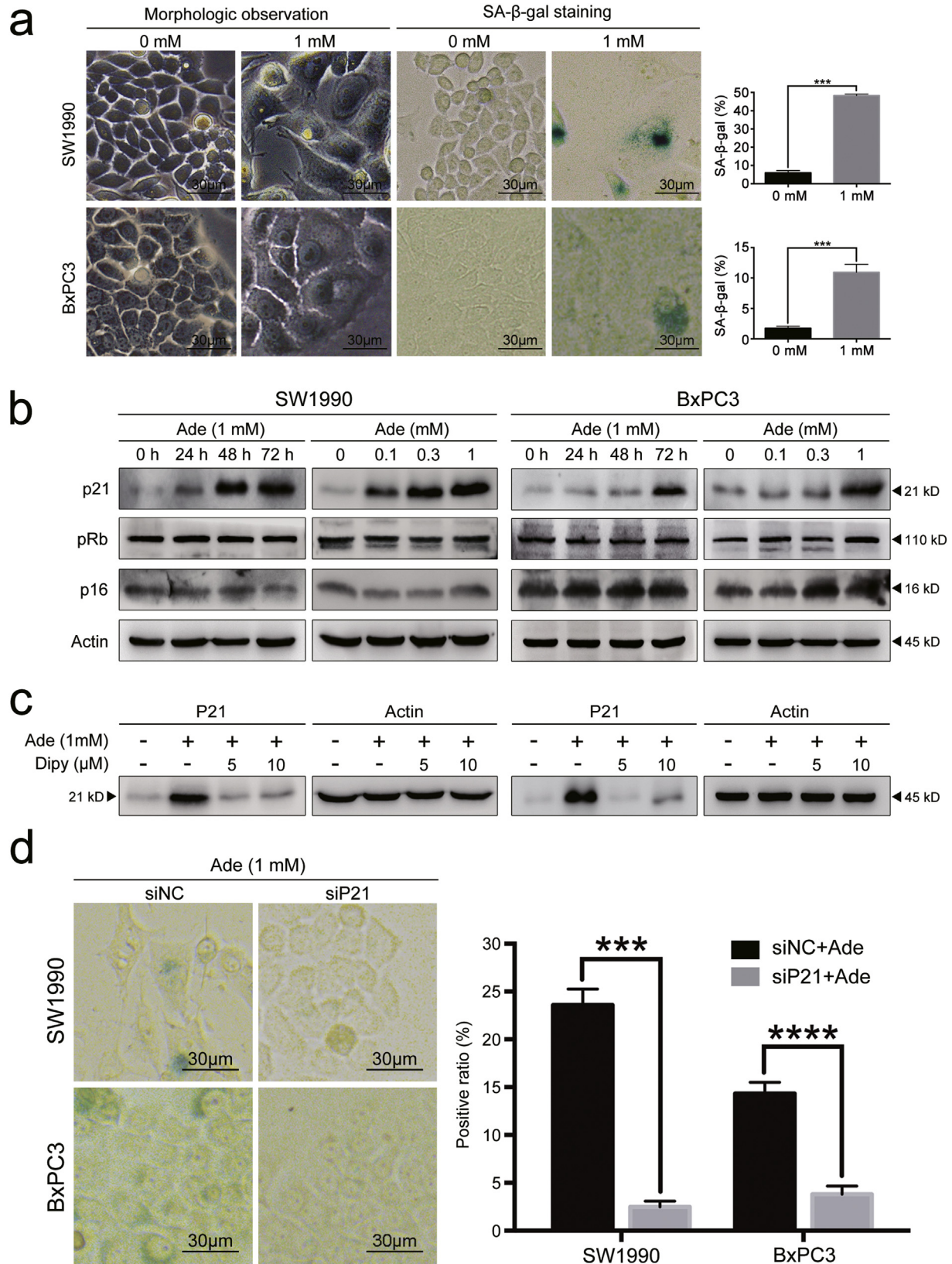


Fig. 4. Adenosine promotes senescence via p21. **a:** The senescent pancreatic cancer cells after a 72 h adenosine treatment were detected and counted by SA-β-gal staining (left panel); the senescence proportions plotted as histograms (right panel). **b:** The protein levels of p21, pRb and p16 analysed by immunoblotting. **c:** The protein levels of p21 from SW1990 and BxPC3 cells receiving a combined treatment of adenosine and dipyrindamole, analysed by immunoblotting. **d:** The senescent SW1990 and BxPC3 cells after p21 silencing and a 72-h adenosine treatment, detected and counted by SA-β-gal staining (left panel); the senescence proportions in the cells with or without p21 silencing, plotted as histograms (right panel); Dipy, dipyrindamole; siNC, non-sense control siRNA; siP21, siRNA for p21. Error bars indicate SEM; *** $P < .001$ and **** $P < .0001$; Student's *t*-test, $n = 3$.

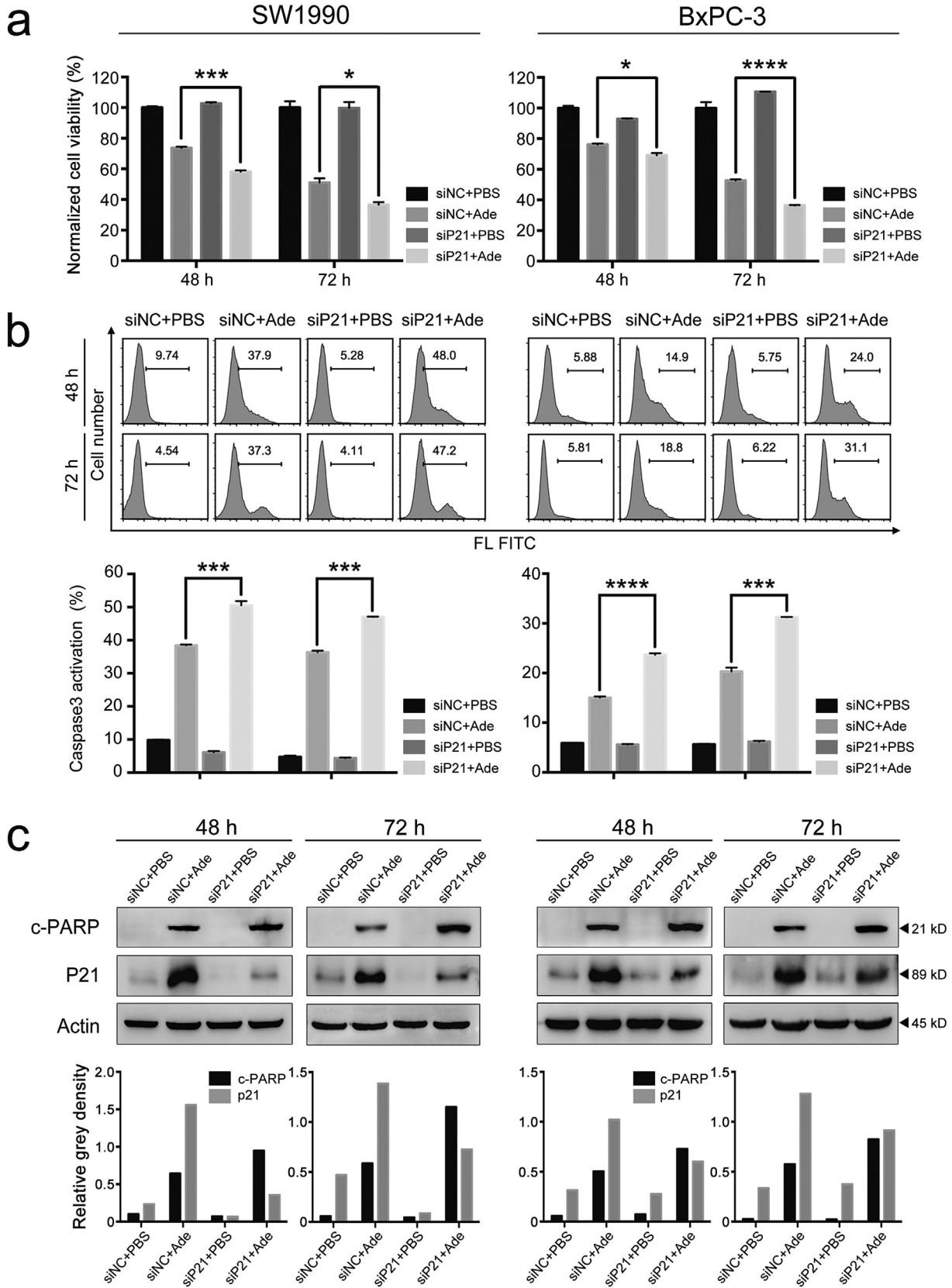
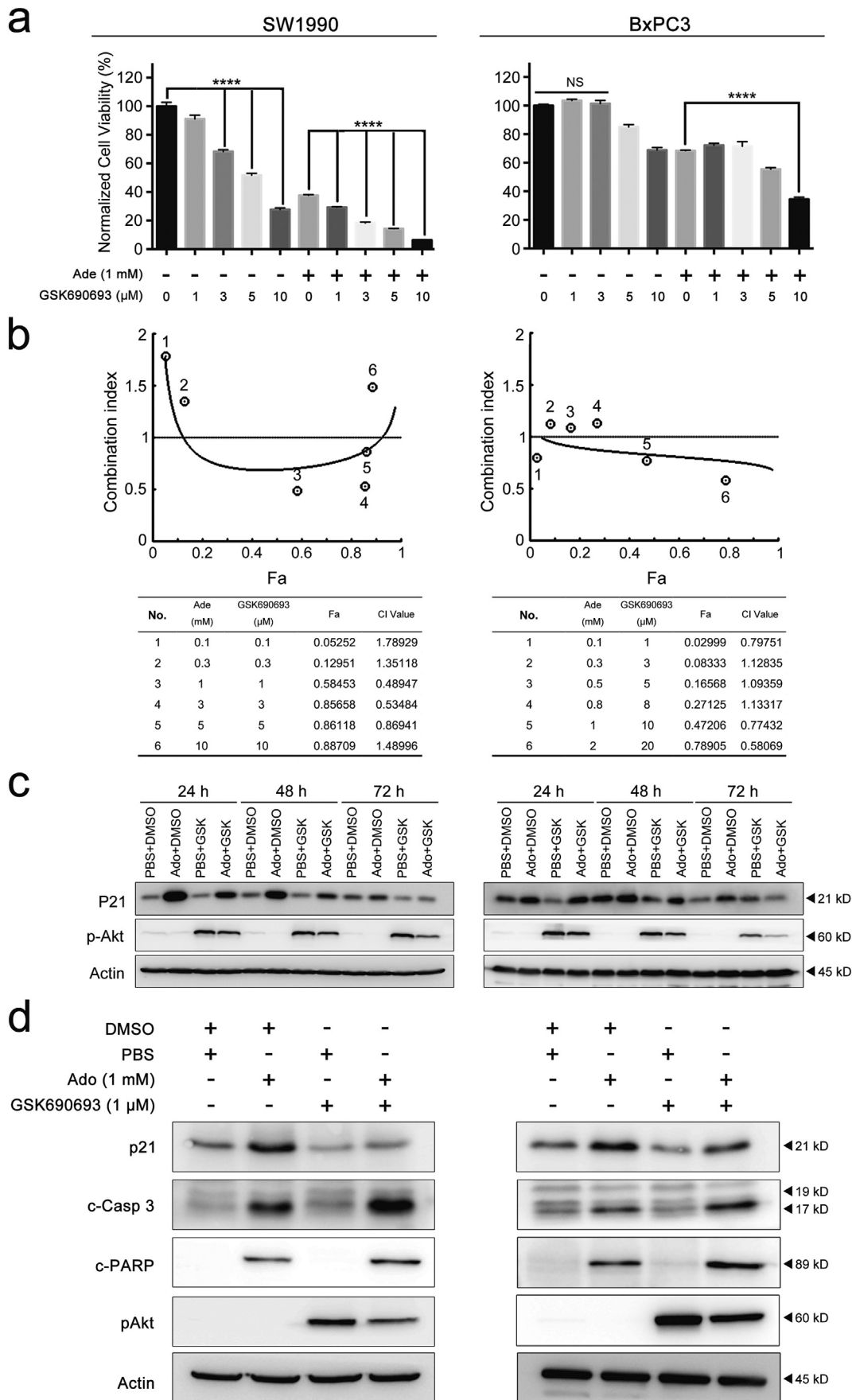


Fig. 5. p21 affects the outcomes of adenosine-treated pancreatic cancer cells. **a:** The cell viability of pancreatic cancer cells with or without p21 silencing, measured by MTS after a 48 h/72 h adenosine treatment. **b:** The caspase-3 cleavage with or without p21 silencing detected and measured by FITC-DEVD-FMK staining (top panel); the relative ratios of the cells with the fluorescent intensity plotted as histograms (bottom panel). **c:** The levels of p21 and PARP cleavage analysed by a combination of p21 silencing and adenosine (top panel); the grey intensities of all bands quantified by ImageJ (bottom panel). Ade, adenosine; siNC, non-sense control siRNA; siP21, siRNA for p21. Error bars indicate SEM; * $P < .05$, *** $P < .001$ and **** $P < .0001$; Student's *t*-test, $n = 3$.



connatural nucleoside induced senescence and apoptosis in pancreatic cancer cells *in vitro*. Utilizing inhibitors for adenosine's catabolic enzymes, or for its receptors, we clarified that in our model adenosine did not function *via* its receptors. Nor was it involved in G-protein-coupled signal transduction followed by cAMP formation and PKA activation in the growth inhibition of pancreatic cancer cells. Instead, we showed that blocking the metabolism by adenosine deaminase inhibitor EHNA exacerbated adenosine-induced cytotoxicity of pancreatic cancer cells, which support acute elevation of intracellular adenosine levels plays a crucial role in this process.

As one of the cytotoxic agents in chemotherapy, adenosine shares the same delivery system as the nucleoside analogue drugs, including gemcitabine and 5-FU [41]. Instead of being passively distributed into tissues, these polar hydrophilic molecules need the assistance of nucleoside transporters for their entrance into cells. Unlike the selective transportation of gemcitabine by ENT1, CNT1, and CNT3 [42], exogenous adenosine can be carried into cells by all members of the equilibrium and concentrative nucleoside transporter families [14]. We have demonstrated in the current study that the concentration of adenosine is important for its suppressive activity in pancreatic cancer cells. We speculate that the expression of ENTs and CNTs might be one of the limiting factors for its potential therapeutic effect. We also found that treatment with adenosine led to increased expression of ENT2, ENT3, and ENT4 in our PDX model, which indicates that adenosine could be a candidate for long-term chemotherapy.

Pancreatic cancers tend to develop strong chemoresistance, which is another obstacle to improving patient prognosis. Recently, “adaptive responses” to chemotherapy, which slow down the cellular proliferation rate but maintain cell viability under environmental stress, have been suggested to be another survival strategy of cancer cells [43,44]. In the current study, we illustrate the antagonizing effect of cellular senescence on apoptosis that was mediated by the Akt-p21 pathway. When the pancreatic cancer cells were treated with a high dose of adenosine, Akt was stimulated to phosphorylate and stabilize p21. p21 accumulation subsequently initiated senescence in the pancreatic cancer cells, blocking apoptotic signal transduction to promote the survival of the cancer cells, in accordance with the known inhibitory functions of p21 against CDK complexes and caspase-3 cleavage [45].

After verifying the anti-tumour effect of adenosine *in vitro* and the mechanism of adenosine treatment resistance in pancreatic cancer cells, we assessed the potential therapeutic value of adenosine alone versus combined treatment with the Akt inhibitor GSK690693 using an EGFP-labelled murine pancreatic cancer orthotopic model. Adenosine and GSK690693 were administered through intraperitoneal injection. The real-time monitoring data of the tumour fluorescent areas suggested that the tumour cell proliferation was significantly suppressed by adenosine, which led to a reduced tumour volume compared with that from the control group after 42 days of treatment. Meanwhile, the addition of GSK690693 to adenosine administration further amplified the potential therapeutic effect of adenosine. Analysis of the tumour tissues also revealed that GSK690693 and adenosine synergistically induced caspase-3 activation and Ki-67 downregulation. These results further support our *in vitro* findings that adenosine induces apoptosis in pancreatic cancers, and GSK690693 can exert sensitizing effects when applied in combination with adenosine.

Since adenosine strongly affects various physiological activities, its probable adverse effects are unavoidable in clinical applications. In the current PDX mice and orthotopic models, adenosine and its co-

therapy with GSK690693 did not cause any significant differences in the average body weight between the treated groups and the control group. As indicated by the blood biochemical tests, the function of the liver, kidney and cardiac muscle remained at normal levels after drug administration (Supplementary Fig. 3). Moreover, adenosine significantly prolonged the overall survival period of the PDX mice in comparison with saline treated animals. These findings indicate that adenosine might result in a better prognosis of pancreatic cancer patients after long-term treatment. Additionally, the synergistic effect of GSK690693 and adenosine suggest that it is possible to further reduce the therapeutic dosage and potential risk of adenosine in clinical applications. Collectively, our findings provide a strong rationale for the administration of adenosine and GSK690693, characterized by low dosage and low toxicity, as a promising potential alternative to the current agents used in pancreatic cancer chemotherapy.

Funding

The work is supported by the grant of the National Natural Science Foundation of China on Dongqin Yang (81572336, 81770579) and Jie Liu (81630016, 81830080), and jointly by the Development Fund for Shanghai Talents (201660). No founders played any role in study design, data collection, data analysis, interpretation, writing of the manuscript; None of any founders had any role in writing the manuscript nor the decision to submit for publication.

Data statement

The datasets generated from the patients during the current study are not publicly available in accordance with local health research ethics protocols but may be available from the corresponding author.

Authors' contributions

Dongqin Yang is mainly responsible for the study concept and design, and critical revision of the manuscript for important intellectual content; Qi Zhang is mainly responsible for acquisition of data and drafting of the manuscript; Zhihui Che is mainly responsible for analysis and interpretation of data; Yunfang Ma is mainly responsible for acquisition of data; Mengmeng Wu is mainly responsible for statistical analysis; Wenli Zhang is mainly responsible for technical support; Lijun Wu is mainly responsible for statistical analysis; Fuchen Liu is mainly responsible for acquisition of data; Wei Xu is mainly responsible for polish the article; Chunhua Song and Mary McGrath are mainly responsible for manuscript editing and writing. Yiwei Chu and Jie liu are mainly responsible for obtained funding and study supervision.

Ethics statement

All animal experiments were performed in accordance with the animal protocols approved by the Institutional Animal Care and Use Committee of Anti-Cancer Biotech (Beijing, China). Prior written informed consents from all patients in accordance with the Declaration of Helsinki and the approval from the Ethics Committee of Fudan University Huashan Hospital were obtained.

Declaration of Competing Interest

The authors declare they have no conflicts of interest.

Fig. 6. The Akt inhibitor GSK690693 synergistically sensitizes pancreatic cancer cells to the cytotoxicity of adenosine by downregulating p21. **a:** The cell viability measured by MTS after adenosine combined with GSK690693 at the indicated concentrations. **b:** The fraction (Fa) of the cells affected by adenosine, GSK690693 or their combinations at the indicated concentrations, measured by MTS after a 72 h treatment; the combination indexes of two drugs calculated (bottom panel) and plotted with Fa (top panel) based on the Chou-Talalay equation. **c:** The protein levels of p21 and pAkt were analysed by immunoblotting in the cells treated by adenosine, GSK690693 or their combinations for 24–72 h. **d:** The protein level of p21, caspase-3 cleavage or PARP cleavage analysed in the cells treated by adenosine, GSK690693 or their combinations for 24–72 h. Ade, adenosine; CI, combination index. Error bars indicate SEM; *****P* < .0001; Student's *t*-test, *n* = 3. NS stands for non-significant.

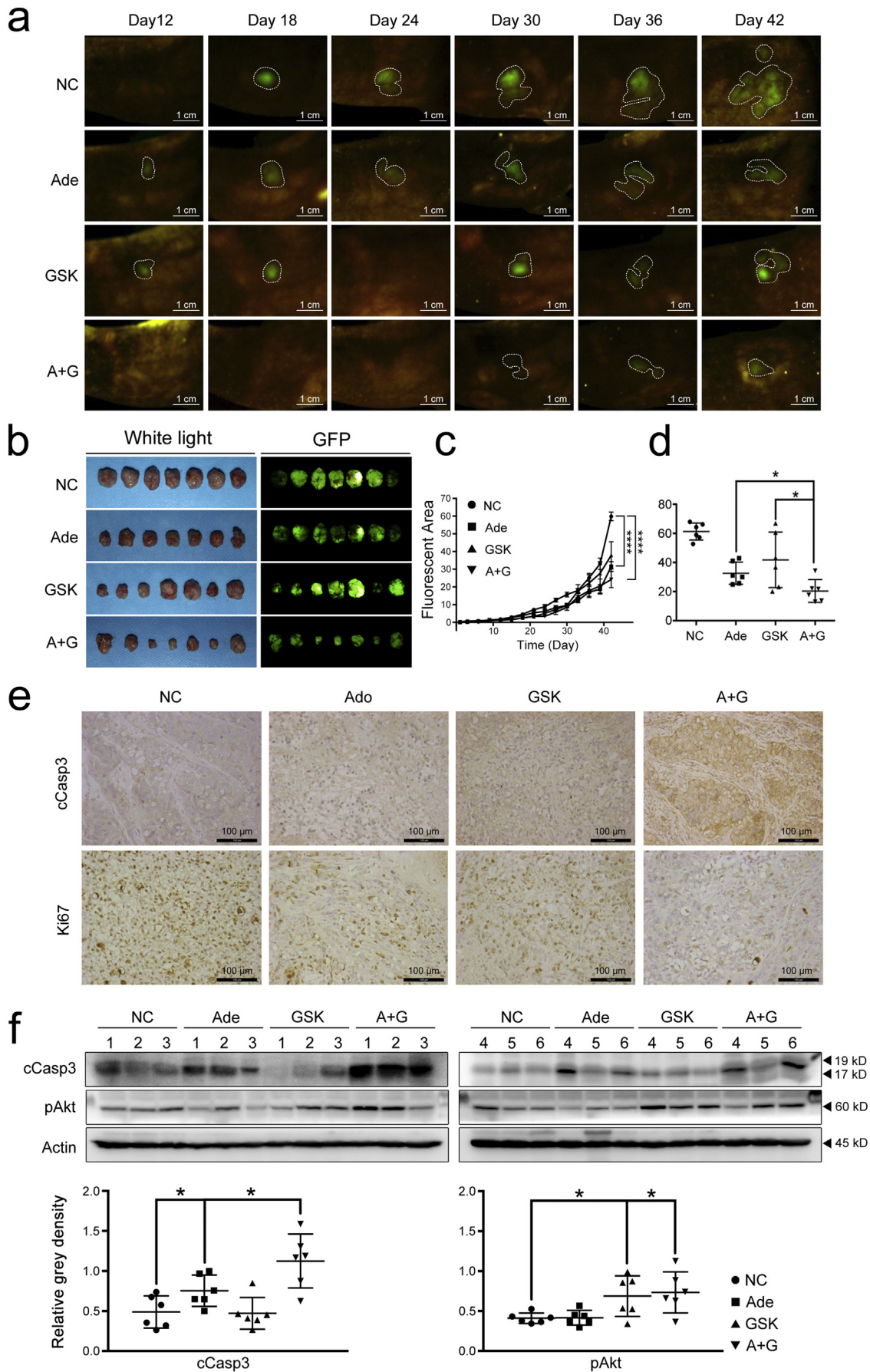


Fig. 7. GSK690693 augments the therapeutic effect of adenosine on pancreatic cancer *in vivo*. **a & c:** The growth rates of tumours monitored and measured based on the fluorescent area in the orthotopic transplantation models treated by adenosine, GSK690693 or their combination from Day 12 to Day 42. Error bars indicate SEM; **** $P < .0001$; two-way ANOVA, $n = 7$. **b & d:** The outcomes of each treatment assessed by the fluorescent area of the tumour issues peeled from the pancreas of the treated mice. **e:** The caspase-3 cleavage and Ki-67 measured by IHC. **f:** The caspase-3 cleavage and phosphorylated Akt in the tumour tissues from all treated mice, analysed by immunoblotting (top panel) and quantified by the grey intensity of the bands (bottom panel). Ade, adenosine; GSK, GSK690693; cCasp3, cleaved caspase-3; pAkt, phosphorylated Akt. Error bars indicate the SEM; * $P < .05$; Student's *t*-test, $n = 7$. NS stands for non-significant.

Acknowledgements

Not applicable.

Appendix A. Supplementary data

Supplementary data to this article can be found online at <https://doi.org/10.1016/j.ebiom.2019.08.068>.

References

- [1] Kamisawa T, Wood LD, Itoi T, Takaori K. Pancreatic cancer. *The Lancet* 2016;388(10039):73–85.
- [2] Ryan DP, Hong TS, Bardeesy N. Pancreatic adenocarcinoma. *N Engl J Med* 2014;371(11):1039–49.
- [3] Siegel RL, Naishadham D, Jemal A. Cancer statistics, CA. *Cancer J Clin* 2013;63(1):11–30.
- [4] Carmichael J, Fink U, Russel RC, Spittle MF, Harris AL, Spiess G, et al. Phase II study of gemcitabine in patients with advanced pancreatic cancer. *Br J Cancer* 1996;73:101–5.
- [5] Burris HA, Moore MJ, Andersen J, Green MR, Rothenberg ML, Modiano MR, et al. Improvement in survival and clinical benefit with gemcitabine as first line therapy for patients with advanced pancreatic cancer: a randomised trial. *J Clin Oncol* 1997;15:2403–13.
- [6] Burris 3rd HA, Moore MJ, Andersen J, Green MR, Rothenberg ML, Modiano MR, et al. Improvements in survival and clinical benefit with gemcitabine as first-line therapy for patients with advanced pancreas cancer: a randomized trial. *J Clin Oncol* 1997;15(6):2403–13.
- [7] Garrido-Laguna I, Hidalgo M. Pancreatic cancer: from state-of-the-art treatments to promising novel therapies. *Nat Rev Clin Oncol* 2015;12(6):319–34.
- [8] Robinson Jr DW, Eisenberg DF, Cella D, Zhao N, de Boer C, DeWitte M. The prognostic significance of patient-reported outcomes in pancreatic cancer cachexia. *J Support Oncol* 2008;6(6):283–90.
- [9] Binenbaum Y, Na'ara S, Gil Z. Gemcitabine resistance in pancreatic ductal adenocarcinoma. *Drug Resist Updat* 2015;23:55–68.
- [10] Palam LR, Gore J, Craven KE, Wilson JL, Korc M. Integrated stress response is critical for gemcitabine resistance in pancreatic ductal adenocarcinoma. *Cell Death Dis* 2015;6:e1913.
- [11] Sheikh R, Walsh N, Clynes M, O'Connor R, McDermott R. Challenges of drug resistance in the management of pancreatic cancer. *Expert Rev Anticancer Ther* 2010;10(10):1647–61.
- [12] Ham J, Evans BA. An emerging role for adenosine and its receptors in bone homeostasis. *Front Endocrinol (Lausanne)* 2012;3:113.
- [13] Antonioli L, Colucci R, Pellegrini C, Giustarini G, Tuccori M, Blandizzi C, et al. The role of purinergic pathways in the pathophysiology of gut diseases: pharmacological modulation and potential therapeutic applications. *Pharmacol Ther* 2013;139(2):157–88.
- [14] Thorn JA, Jarvis SM. Adenosine transporters. *Gen Pharmacol* 1996;27(4):613–20.
- [15] Borea PA, Varani K, Vincenzi F, Baraldi PG, Tabrizi MA, Merighi S, et al. The A3 adenosine receptor: history and perspectives. *Pharmacol Rev* 2015;67(1):74–102.
- [16] Acurio J, Troncoso F, Bertoglia P, Salomon C, Aguayo C, Sobrevia L, et al. Potential role of A2B adenosine receptors on proliferation/migration of fetal endothelium derived from preeclamptic pregnancies. *Biomed Res Int* 2014;2014:274507.
- [17] Gessi S, Merighi S, Stefanelli A, Fazzi D, Varani K, Borea PA. A(1) and A(3) adenosine receptors inhibit LPS-induced hypoxia-inducible factor-1 accumulation in murine astrocytes. *Pharmacol Res* 2013;76:157–70.
- [18] Novitskiy SV, Ryzhov S, Zaynagetdinov R, Goldstein AE, Huang Y, Tikhomirov OY, et al. Adenosine receptors in regulation of dendritic cell differentiation and function. *Blood* 2008;112(5):1822–31.
- [19] Yu S, Hou D, Chen P, Zhang Q, Lv B, Ma Y, et al. Adenosine induces apoptosis through TNFR1/RIPK1/P38 axis in colon cancer cells. *Biochem Biophys Res Commun* 2015;460(3):759–65.
- [20] Ma Y, Zhang J, Zhang Q, Chen P, Song J, Yu S, et al. Adenosine induces apoptosis in human liver cancer cells through ROS production and mitochondrial dysfunction. *Biochem Biophys Res Commun* 2014;448(1):8–14.
- [21] Saitoh M, Nagai K, Nakagawa K, Yamamura T, Yamamoto S, Nishizaki T. Adenosine induces apoptosis in the human gastric cancer cells via an intrinsic pathway relevant to activation of AMP-activated protein kinase. *Biochem Pharmacol* 2004;67(10):2005–11.
- [22] Fishman P, Bar-Yehuda S, Ohana G, Pathak S, Wasserman L, Barer F, et al. Adenosine acts as an inhibitor of lymphoma cell growth: a major role for the A3 adenosine receptor. *Eur J Cancer* 2000;36(11):1452–8.
- [23] Yang D, Yaguchi T, Lim CR, Ishizawa Y, Nakano T, Nishizaki T. Tuning of apoptosis-mediator gene transcription in HepG2 human hepatoma cells through an adenosine signal. *Cancer Lett* 2010;291(2):225–9.
- [24] Tamura K, Kanno T, Fujita Y, Gotoh A, Nakano T, Nishizaki T. A(2a) adenosine receptor mediates HepG2 cell apoptosis by downregulating Bcl-X(L) expression and up-regulating Bid expression. *J Cell Biochem* 2012;113(5):1766–75.
- [25] Yang D, Yaguchi T, Nagata T, Gotoh A, Dovat S, Song C, et al. AMID mediates adenosine-induced caspase independent HuH-7 cell apoptosis. *Cell Physiol Biochem* 2011;27(7).
- [26] Yang D, Li L, Liu H, Wu L, Luo Z, Li H, et al. Induction of autophagy and senescence by knockdown of ROC1 E3 ubiquitin ligase to suppress the growth of liver cancer cells. *Cell Death Differ* 2013;20(2):235–47.
- [27] Jun E, Jung J, Jeong SY, Choi EK, Kim MB, Lee JS, et al. Surgical and oncological factors affecting the successful engraftment of patient-derived Xenografts in pancreatic ductal adenocarcinoma. *Anticancer Res* 2016;36(2):517–21.
- [28] Garrido-Laguna I, Uson M, Rajeshkumar NV, Tan AC, de Oliveira E, Karikari C, et al. Tumor engraftment in nude mice and enrichment in stroma-related gene pathways predict poor survival and resistance to gemcitabine in patients with pancreatic cancer. *Clin Cancer Res* 2011;17(17):5793–800.
- [29] Hoffman RM, Yang M. Whole-body imaging with fluorescent proteins. *Nat Protoc* 2006;1(3):1429–38.
- [30] Hasegawa K, Suetsugu A, Nakamura M, Matsumoto T, Aoki H, Kunisada T, et al. Imaging the role of multinucleate pancreatic Cancer cells and Cancer-associated fibroblasts in peritoneal metastasis in mouse models. *Anticancer Res* 2017;37(7):3435–40.
- [31] Sai K, Yang D, Yamamoto H, Fujikawa H, Yamamoto S, Nagata T, et al. A(1) adenosine receptor signal and AMPK involving caspase-9/–3 activation are responsible for adenosine-induced RCR-1 astrocytoma cell death. *Neurotoxicology* 2006;27(4):458–67.
- [32] Noji T, Karasawa A, Kusaka H. Adenosine uptake inhibitors. *Eur J Pharmacol* 2004;495(1):1–16.
- [33] Murray AJ. Pharmacological PKA inhibition: all may not be what it seems. *Sci Signal* 2008;1(22):re4.
- [34] Li Y, Dowbenko D, Lasky LA. AKT/PKB phosphorylation of p21Cip/WAF1 enhances protein stability of p21Cip/WAF1 and promotes cell survival. *J Biol Chem* 2002;277(13):11352–61.
- [35] Zhou BP, Liao Y, Xia W, Spohn B, Lee MH, Hung MC. Cytoplasmic localization of p21Cip1/WAF1 by Akt-induced phosphorylation in HER-2/neu-overexpressing cells. *Nat Cell Biol* 2001;3(3):245–52.
- [36] Zhan J, Easton JB, Huang S, Mishra A, Xiao L, Lacy ER, et al. Negative regulation of ASK1 by p21Cip1 involves a small domain that includes Serine 98 that is phosphorylated by ASK1 in vivo. *Mol Cell Biol* 2007;27(9):3530–41.
- [37] Abbas T, Dutta A. p21 in cancer: intricate networks and multiple activities. *Nat Rev Cancer* 2009;9(6):400–14.
- [38] Panupinthu N, Yu S, Zhang D, Zhang F, Gagea M, Lu Y, et al. Self-reinforcing loop of amphiregulin and Y-box binding protein-1 contributes to poor outcomes in ovarian cancer. *Oncogene* 2014;33(22):2846–56.
- [39] Antonioli L, Blandizzi C, Pacher P, Hasko G. Immunity, inflammation and cancer: a leading role for adenosine. *Nat Rev Cancer* 2013;13(12):842–57.
- [40] Dias RB, Rombo DM, Ribeiro JA, Henley JM, Sebastiao AM. Adenosine: setting the stage for plasticity. *Trends Neurosci* 2013;36(4):248–57.
- [41] Molina-Arcas M, Casado FJ, Pastor-Anglada M. Nucleoside transporter proteins. *Curr Vasc Pharmacol* 2009;7(4):426–34.
- [42] Mackey JR, Yao SY, Smith KM, Karpinski E, Baldwin SA, Cass CE, et al. Gemcitabine transport in xenopus oocytes expressing recombinant plasma membrane mammalian nucleoside transporters. *J Natl Cancer Inst* 1999;91(21):1876–81.
- [43] Ewald JA, Desotelle JA, Wilding G, Jarrard DF. Therapy-induced senescence in cancer. *J Natl Cancer Inst* 2010;102(20):1536–46.
- [44] Gordon RR, Nelson PS. Cellular senescence and cancer chemotherapy resistance. *Drug Resist Updat* 2012;15(1–2):123–31.
- [45] Besson A, Dowdy SF, Roberts JM. CDK inhibitors: cell cycle regulators and beyond. *Dev Cell* 2008;14(2):159–69.